

Radiographic and CT Features of Viral Pneumonia¹

Hyun Jung Koo, MD, PhD

Soyeoun Lim, MD

Jooae Choe, MD

Sang-Ho Choi, MD, PhD

Heungsup Sung, MD

Kyung-Hyun Do, MD, PhD

Abbreviations: CMV = cytomegalovirus, GGO = ground-glass opacity, HMPV = human metapneumovirus, HPIV = human parainfluenza virus, HSV = herpes simplex virus, MERS = Middle East respiratory syndrome, RSV = respiratory syncytial virus, SARS = severe acute respiratory syndrome

RadioGraphics 2018; 38:719–739

<https://doi.org/10.1148/rg.2018170048>

Content Codes: CH CT

¹From the Department of Radiology and Research Institute of Radiology (H.J.K., J.C., K.H.D.), Division of Infectious Disease, Department of Internal Medicine (S.H.C.), and Department of Laboratory Medicine (H.S.), Asan Medical Center, University of Ulsan College of Medicine, Olympic-ro 43-gil, Songpa-gu, 05505 Seoul, South Korea; and Department of Radiology, Ulsan University Hospital, Ulsan University College of Medicine, Ulsan, South Korea (S.L.). Presented as an education exhibit at the 2016 RSNA Annual Meeting. Received March 11, 2017; revision requested May 18 and received August 6; accepted August 11. For this journal-based SA-CME activity, the authors, editor, and reviewers have disclosed no relevant relationships. **Address correspondence to** K.H.D. (e-mail: dokh@amc.seoul.kr).

©RSNA, 2018

SA-CME LEARNING OBJECTIVES

After completing this journal-based SA-CME activity, participants will be able to:

- Identify radiographic and characteristic CT patterns of viral pneumonia according to pathogen.
- Review new viruses including HMPV, SARS coronavirus, MERS coronavirus, and H1N1 virus.
- Discuss the clinical characteristics of viral pneumonia such as patient age and immune status, seasonal variation, and community outbreak periods.

See www.rsna.org/education/search/RG.

An earlier incorrect version of this article appeared online. This article was corrected on September 10, 2018.

Viruses are the most common causes of respiratory infection. The imaging findings of viral pneumonia are diverse and overlap with those of other nonviral infectious and inflammatory conditions. However, identification of the underlying viral pathogens may not always be easy. There are a number of indicators for identifying viral pathogens on the basis of imaging patterns, which are associated with the pathogenesis of viral infections. Viruses in the same viral family share a similar pathogenesis of pneumonia, and the imaging patterns have distinguishable characteristics. Although not all cases manifest with typical patterns, most typical imaging patterns of viral pneumonia can be classified according to viral families. Although a definite diagnosis cannot be achieved on the basis of imaging features alone, recognition of viral pneumonia patterns may aid in differentiating viral pathogens, thus reducing the use of antibiotics. Recently, new viruses associated with recent outbreaks including human metapneumovirus, severe acute respiratory syndrome coronavirus, and Middle East respiratory syndrome coronavirus have been discovered. The imaging findings of these emerging pathogens have been described in a few recent studies. This review focuses on the radiographic and computed tomographic patterns of viral pneumonia caused by different pathogens, including new pathogens. Clinical characteristics that could affect imaging, such as patient age and immune status, seasonal variation and community outbreaks, and pathogenesis, are also discussed. The first goal of this review is to indicate that there are imaging features that should raise the possibility of viral infections. Second, to help radiologists differentiate viral infections, viruses in the same viridae that have similar pathogenesis and can have similar imaging characteristics are shown. By considering both the clinical and radiologic characteristics, radiologists can suggest the diagnosis of viral pneumonia.

©RSNA, 2018 • radiographics.rsna.org

Introduction

Viruses are the most common causes of acute respiratory infections, and causative agents of lower respiratory tract infection vary according to patient age and immunity (Table 1). Computed tomographic (CT) findings of viral pneumonia are diverse and may be affected by the immune status of the host and the underlying pathophysiology of the viral pathogen. Moreover, coinfection with bacteria is common. In a previous study, Pavia (1) suggested that biphasic patterned illness, consolidation on chest radiographs, and high inflammation markers may increase the likelihood of bacterial coinfection (1).

The clinical and CT findings of numerous respiratory viral pathogens such as influenza, human parainfluenza virus (HPIV), respiratory syncytial virus (RSV), rhinovirus, and adenovirus have been described (1,2). RSV shows an airway-centric pattern of disease with

TEACHING POINTS

- Adenovirus pneumonia shows bilateral multifocal GGO with patchy consolidations on CT images and may show lobar or segmental distribution indicative of bronchopneumonia that resembles bacterial pneumonia.
- At CT, HPIV pneumonia shows multifocal patchy consolidation with GGO that hinders differentiation of viral from bacterial pneumonia, and approximately one-fourth of patients show centrilobular nodules with bronchial wall thickening.
- Radiographs in patients with HMPV pneumonia show multilobar infiltrations. CT findings in immunocompetent patients with HMPV pneumonia have not been described yet; however, bilateral ill-defined centrilobular nodules, branching centrilobular nodules, and GGO are noted in patients with hematologic malignancy.
- Radiographs in patients with influenza pneumonia show bilateral reticulonodular areas of opacity with or without focal areas of consolidation, usually in the lower lobes. Poorly defined patchy or nodular areas of consolidation that become rapidly confluent and represent either diffuse alveolar damage or superinfection are seen frequently and resolve in 3 weeks.
- MERS pneumonia appears on CT images as subpleural and basilar airspace lesions, with extensive GGO and consolidation. Cavitation is uncommon.

“tree-in-bud” opacity and bronchial wall thickening. Adenovirus appears as multifocal consolidation or ground-glass opacity (GGO), and GGO was more frequently noticed in patients with adenovirus pneumonia than in those with other viral infections or bacterial infections. A diffuse airspace pattern was seen more frequently in patients with bacterial infections. On the basis of the imaging patterns of pneumonia, we can suggest a differential diagnosis of the pathogen during early stages of the infection. Diagnostic tests including radiologic studies and blood or serologic tests that could help establish the cause of pneumonia would reduce the use of antibiotics and may improve the clinical course. Moreover, rapid diagnosis can lead to early control of potential transmission, thus decreasing overall treatment costs.

With the recent advancement in molecular biology and the ability to amplify multiple viral genomes by using multiplex reverse-transcription polymerase chain reaction assays, several new human respiratory viruses, such as human metapneumovirus (HMPV), human coronaviruses, and bocavirus have been discovered (3,4). A number of these new viruses, including severe acute respiratory syndrome (SARS) coronavirus and Middle East respiratory syndrome (MERS) coronavirus, have been associated with regional outbreaks in the past and could reemerge to produce outbreaks in the future (5). In this review, we focus on the radiographic and CT patterns of viral pneumonia according to pathogens, includ-

ing newly identified viral organisms, and discuss clinical characteristics such as age, immune status, seasonal variation in incidence, and community outbreak periods of specific infections.

Pathogenesis of Viral Pneumonia

CT patterns of viral pneumonia are related to the pathogenesis of pulmonary viral infection (Table 2). Although not all cases demonstrate typical imaging patterns, most viral pneumonia patterns exhibit similarity on the basis of viridae (Fig 1). For example, RSV and HPIV replicate in the nasopharyngeal epithelium, spread to the lungs, and induce bronchiolitis with sloughing of epithelial cells of the small airways (6). HMPV also infects the lung epithelium and induces an inflammatory cascade (7). The CT findings of RSV pneumonia, HPIV pneumonia, and HMPV pneumonia are similar. The viruses usually appear as multifocal patchy consolidation with GGO, and centrilobular nodules with bronchial wall thickening are also noticed. Influenza virus diffusely invades the respiratory epithelium, resulting in necrotizing bronchitis and diffuse alveolar damage, which manifest as consolidation (8). Adenovirus affects the terminal bronchioles and causes bronchiolitis, which may be accompanied by necrotizing bronchopneumonia. Herpes simplex virus (HSV) has cytopathic effects in both the airways and alveoli; these manifest as a multifocal scattered airspace pattern of opacity and predominant areas of peribronchial consolidation. Intranuclear inclusions can be observed in lung biopsy tissue or at cytologic examination of bronchoalveolar lavage fluid. In a patient with HSV pneumonia who underwent open lung biopsy, areas of GGO on CT images corresponded to pathologic diffuse alveolar damage (9). The presence of mononuclear or multinuclear epithelial cells containing an intranuclear inclusion suggests the diagnosis of HSV pneumonia. Similarly, cytomegalovirus (CMV) exhibits acute interstitial pneumonia with diffuse alveolar edema with fibrinous exudate. Multifocal nodular infiltration represents infected areas of cells with cytoplasmic CMV inclusion. In a murine model of CMV pneumonia, interstitial fibrocytes, alveolar epithelial cells, and endothelial cells were target cells of CMV infection (10).

Adenoviridae

Human Adenovirus

Adenovirus is a double-stranded DNA virus with more than 50 identified serotypes that account for 5%–10% of all respiratory tract infections in children (11). It can cause respiratory epithelial cell lysis and effects distal to terminal bronchioles. Patients present with pharyngitis, laryn-

Table 1: Lower Respiratory Tract Viral Infections in Children and Adults

Pediatric	
Immunocompetent	
	RSV
	HPIV
	Influenza
	HMPV
	Adenovirus
	Rhinovirus
Immunocompromised	
	Adenovirus
	CMV
	Epstein-Barr virus
	HSV
	RSV
Adult	
Immunocompetent	
	Influenza
	HPIV
	Adenovirus
	RSV
	HMPV
Immunocompromised	
	Influenza
	RSV
	Adenovirus
	Rhinovirus
	HPIV
	HMPV
	Coronavirus
	CMV
	HSV
	Varicella-zoster virus
	Human bocavirus

Note.—CMV = cytomegalovirus, HPIV = human parainfluenza virus, HMPV = human metapneumovirus, HSV = herpes simplex virus, RSV = respiratory syncytial virus.

gotracheobronchitis, bronchiolitis, or bronchopneumonia. In most immunocompetent patients, adenovirus pneumonia is mild, is associated with upper respiratory symptoms, and resolves within 2 weeks. Monocytopenia, multilobar infiltration, and pleural effusion are associated with respiratory failure in immunocompetent adults (12). Community outbreaks of adenovirus infection have been reported, and severe cases caused by adenovirus serotype 14 have been associated with older age, chronic underlying conditions, and low absolute lymphocyte counts (13,14). Adenovirus infection exhibits more severe and fatal condi-

tions with acute respiratory distress syndrome in immunocompromised patients. An adenovirus infection occurs in 10.5% of patients undergoing hematopoietic stem cell transplantation; younger age, alternative donor grafts, and acute graft-versus-host disease are risk factors for infection (15).

Adenovirus pneumonia shows bilateral multifocal GGO with patchy consolidations on images and may show lobar or segmental distribution indicative of bronchopneumonia (Fig 2) that resembles bacterial pneumonia. Hyperinflation and lobar atelectasis are common in infants and children. Long-term sequelae of adenovirus pneumonia, such as bronchiectasis, bronchiolitis obliterans, and unilateral hyperlucent lung (Swyer-James-MacLeod) syndrome, could be combined.

Herpesviridae

Human herpesviruses are large DNA viruses that can cause either primary (acute) or nonprimary (chronic or latent) infection. Herpesviridae have the ability to remain latent in tissue after the acute infection has resolved and can be reactivated by internal and external triggers. There are a number of severe pathogenic human herpesviruses including HSV types 1 and 2, varicella-zoster virus, Epstein-Barr virus, CMV, and herpesviruses 6 and 7. Respiratory tract infection caused by herpesviridae has been demonstrated after primary infection and reactivation. Clinically diagnosed infections have been described in both immunocompetent and immunocompromised patients. Lung involvement of HSV-1, HSV-2, Epstein-Barr virus, and CMV has been demonstrated predominantly in immunocompromised hosts.

HSV Pneumonia

HSV pneumonia is caused predominately by HSV type 1 and rarely by HSV type 2 (16,17). HSV type 1 pneumonia is uncommon, usually localized, and well tolerated in healthy individuals; however, it is observed in immunocompromised patients or individuals whose airways have been traumatized by intubation, smoke inhalation, or chronic cigarette smoking (18). Predisposing host factors include severe burns, acquired immunodeficiency syndrome (AIDS), malignancy, organ transplantation, trauma from intubation, smoke inhalation, and chronic cigarette smoking (19). Primary HSV infection occurs by means of close personal contact through saliva or cutaneous or oral vesicle fluid, which can cause gingivostomatitis in children and herpes labialis in adults. There are two possible routes for lower respiratory tract involvement: aspiration or extension of oropharyngeal infection into the lower respiratory system and

Table 2: Pathogenesis and CT Findings of Viral Pneumonia

Family [subfamily]	Common Name	Transmission*	Pathogenesis	Typical CT Findings						Systemic Involvement
				Distribution	Consolidation	GGO	Nodule	Bronchial Wall Thickening	Pleural Effusion	
Adeno-	Adenovirus	Respiratory, fecal-oral, conjunctival	Bronchiolar and alveolar damage	Multifocal	+++	+++	Centrilobular+	UC	C	Not definite
Herpes- [Alphaherpes-]	HSV	Contact (oral or genital secretion)	Cytopathic effect with diffuse alveolar damage	Multifocal random, or segmental	++	+++	+	UC	F	Gingivostomatitis, pharyngitis and herpes labialis (HSV1)
	Varicella-zoster virus	Contact, airborne (aerosol, droplets)	Hematogenous spread to alveolus, cytopathic effect with mononuclear cell infiltration	Multifocal	Rare	Surrounding halo	1-10 mm (in late phase, calcification)	UC	Rare	Skin rash
Herpes- [Betaherpes-]	CMV	Contact, transfusional, blood transfusion	Cytopathic effect with diffuse alveolar damage	Diffuse	++	++++	++	UC	Rare	Not definite
Herpes- [Gammaherpes-]	Epstein-Barr virus	Oral, blood transfusion, organ transplantation	Mononuclear inflammatory cell infiltration along bronchovascular bundles and interlobular septa	Diffuse	Rare	++	Rare	UC	V	Infectious mononucleosis, mediastinal LAP, splenomegaly
Parvo-[Parvo-]	Bocavirus†	Aerosol and contact	Induced cytokine expression	Diffuse	++	++	Rare	UC	C	Not definite
Paramyxo-	HPV	Contact, droplet	Bronchiolar and alveolar damage with mucus plugging	Airway, multifocal	+	+	Centrilobular++	C	UC	Not definite
	Measles	Airborne (aerosol, droplets), contact with secretion or skin rash	Bronchiolar and alveolar epithelial damage with multinucleated giant cell formation	Multifocal	Rare	+	+	UC	C	Hilar LAP, gastroenteritis, encephalitis
	Mumps†	Droplets or aerosol, transplacental	Mononuclear cell infiltration of bronchiole and alveolar septa	Multifocal	Rare	++	Rare	UC	Rare	Parotid gland (95% of patients)

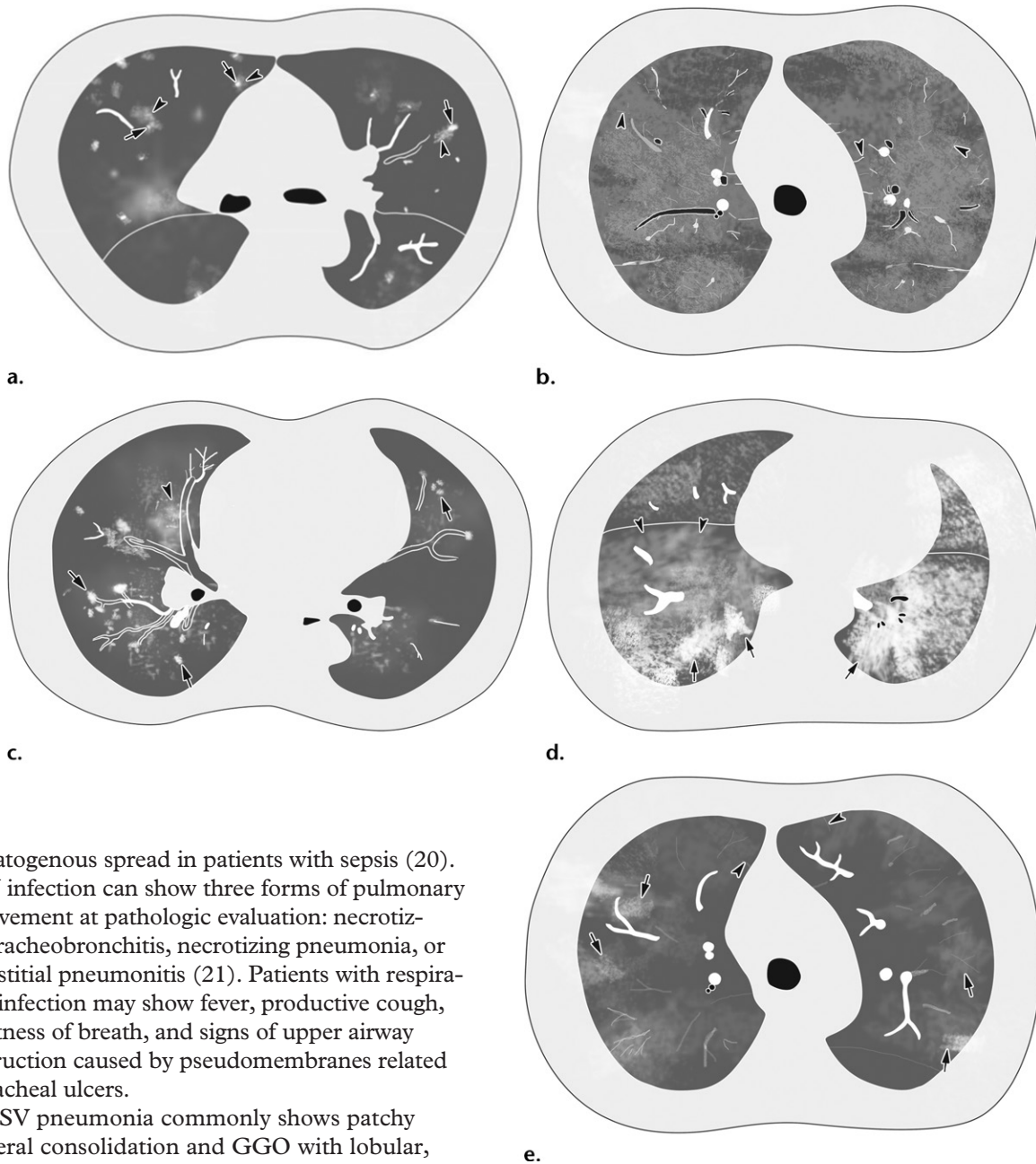
Pneumo-	RSV	Contact, aerosol	Destruction of bronchial and alveolar epithelium with small airway obstruction	Airway, multifocal	+	Centrilobular+++	C	Not definite
	HMPV	Direct or close contact, droplet, aerosol	Upregulation of cytokines leads to perivascular and peribronchiolar infiltration	Airway, multifocal	+	Centrilobular+++	C	Not definite
Hanta-	HCPS, HFRS	Aerosol	Direct involvement of vascular endothelium resulting in increased endothelial permeability	Pulmonary edema	Rare	Rare	UC	ARF (HFRS), thrombocytopenia, hypotension, shock (HCPS)
Phenui-	SFTS	Tick-borne	Upregulation of cytokines resulting in increased endothelial permeability	Pulmonary edema	Rare	Rare	UC	Shock, multiorgan failure, thrombocytopenia
Orthomyxo-	Influenza	Droplet, airborne	Destruction of airway epithelial barrier, resulting in necrotizing bronchitis and diffuse alveolar damage	Airway, multifocal	+	++	C	Not definite
Corona- [Corona-]	Human coronavirus	Droplet, airborne, contact	SARS: diffuse alveolar damage by involving angiotensin-converting enzyme; MERS: dysregulation of the host cellular transcriptome resulting in apoptosis	Peripheral, multifocal	+++	Rare	UC	Not definite
Picorna-	Rhinovirus	Droplet, aerosol, or contact	Disruption of epithelial barrier function causing increase vascular leakage and mucus secretion; no cytopathic effect	Multifocal	+	Rare	UC	Not definite
	Enterovirus	Fecal-oral, contact, droplet	Attachment to decay-accelerating factor of the lower respiratory tract	Multifocal	+	Rare	UC	Not definite

Note.—ARF = acute renal failure, C = common, F = frequent, HCPS = hantavirus cardiopulmonary syndromes, HFRS = hemorrhagic fever with renal syndrome, LAP = lymphadenopathy, SFTS = severe fever with thrombocytopenia syndrome, UC = uncommon, V = variable. Percentage of the area of lung involvement: + = 10%–25%, ++ = 25%–50%, +++ = 50%–75, ++++ = greater than 75%.

*The main routes of transmission are listed first.

†CT findings of Bocavirus pneumonia or pulmonary involvement of mumps are not well established; there are few case reports in the literature.

Figure 1. Schemas show typical CT patterns of viral pneumonia. (a) Pneumonia due to varicella-zoster virus shows multifocal 1–10-mm well-defined or ill-defined nodular opacity (arrows) with a surrounding halo or patchy GGO (arrowheads) in both lungs. (b) Pneumonia due to CMV shows diffuse ill-defined patchy GGO with interlobular septal thickening (arrowheads) in both lungs. (c) Pneumonia due to HMPV shows multiple ill-defined nodules (arrows) or GGO (arrowhead) along the bronchovascular bundles in both lungs. These findings are similar to those of HPIV pneumonia, which belongs to the same *viridae*. (d) Pneumonia due to influenza A virus shows multiple irregular areas of consolidation (arrows) along the bronchovascular bundles and diffuse GGO (arrowheads) with interlobular septal thickening in both lungs. (e) Pneumonia due to rhinovirus shows multiple ill-defined patchy areas of GGO (arrows) with interlobular septal thickening (arrowheads) in both lungs.



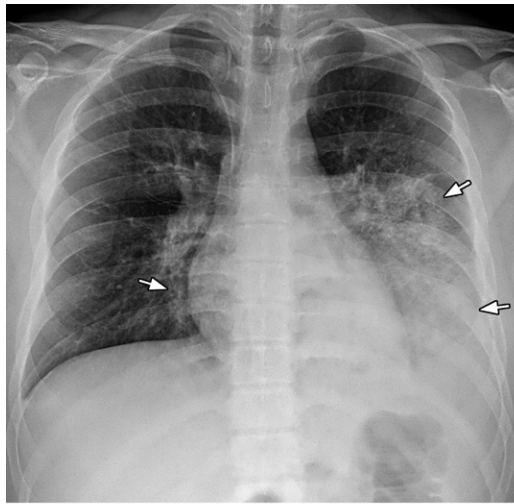
hematogenous spread in patients with sepsis (20). HSV infection can show three forms of pulmonary involvement at pathologic evaluation: necrotizing tracheobronchitis, necrotizing pneumonia, or interstitial pneumonitis (21). Patients with respiratory infection may show fever, productive cough, shortness of breath, and signs of upper airway obstruction caused by pseudomembranes related to tracheal ulcers.

HSV pneumonia commonly shows patchy bilateral consolidation and GGO with lobular, segmental, or subsegmental distribution on chest radiographs (22) (Fig 3a). Reticular opacity also can be present. CT demonstrates predominantly multifocal segmental or subsegmental areas of GGO and less dominant focal areas of consolidation. Pleural effusion is common (16). The presence of small or larger centrilobular nodules is controversial; however, they can be due to viral pneumonia itself, multiple hemorrhagic nodules, or coexisting fungal pneumonia (16,17). No differences have been observed between the CT

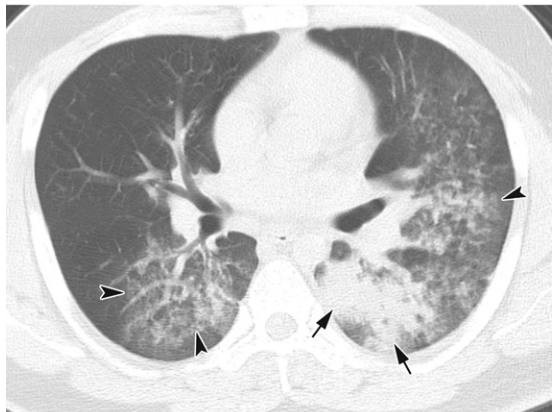
findings of immunocompromised and immunocompetent patients (9).

Varicellovirus (α Herpesvirinae)

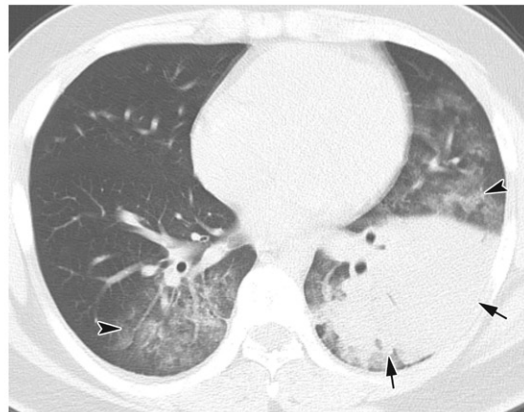
Varicella-zoster virus infection (ie, chickenpox) is usually a self-limited benign disease in children. However, disseminated varicella-zoster virus infection may result in mortality rates of 9%–50%,



a.



b.



c.

Figure 2. Pneumonia due to adenovirus in a 20-year-old man with fever, cough, and dyspnea. (a) Initial chest radiograph shows ill-defined patchy consolidation and GGO (arrows) in the left middle to lower lungs and the right lower lung zone. (b, c) Axial chest CT images (5-mm thickness) obtained on the same day at the interlobar bronchi level (b) and the inferior pulmonary vein level (c) show ill-defined patchy GGO (arrowheads) and lobar consolidations (arrows).

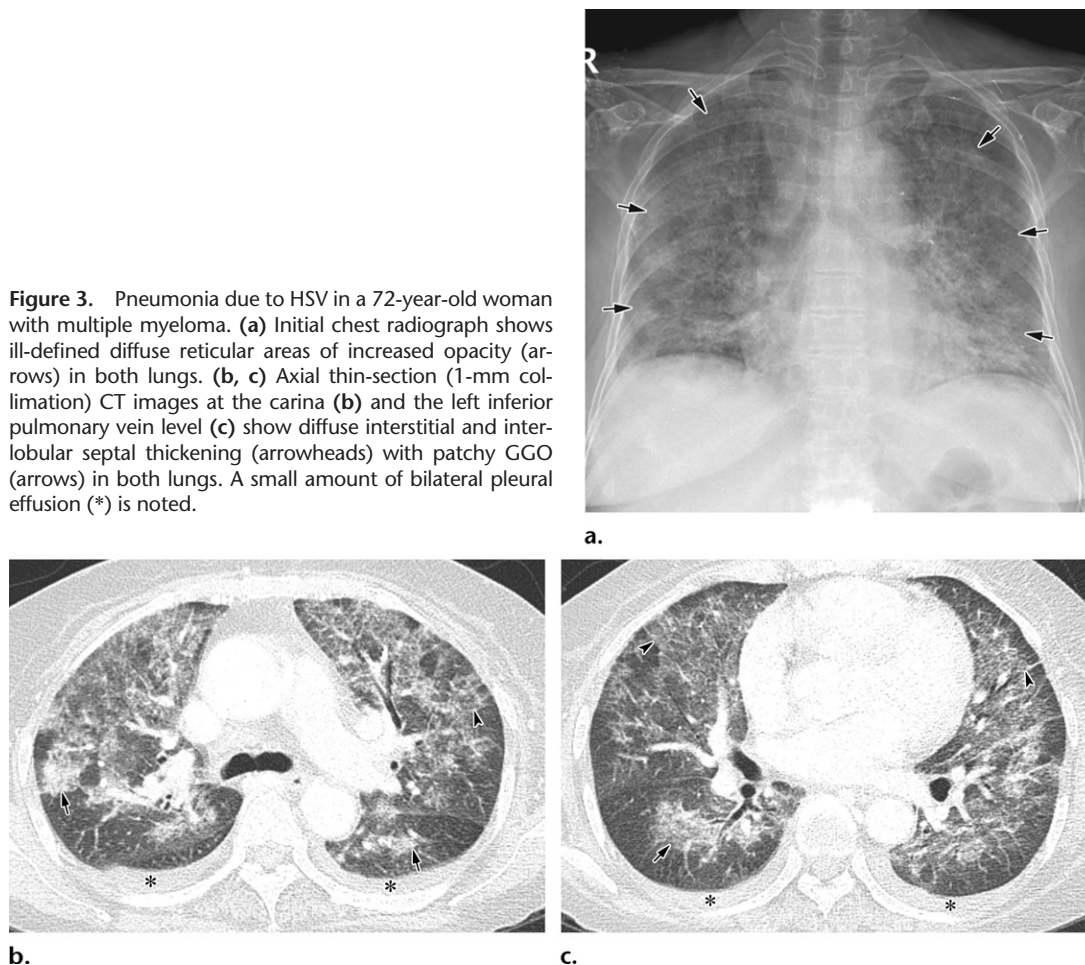
and pneumonia is the most common and serious complication. The risk of disseminated disease increases in patients with lymphoma and in immunocompromised or pregnant patients (23). The diagnosis of varicella infection usually can be established on the basis of clinical findings (rash, pulmonary symptoms, and history of contact with a patient with chickenpox). However, in problematic cases, varicella-zoster serologic evaluation can be performed to confirm the diagnosis. With recovery from the initial disease, spherical nodules are observed scattered randomly throughout the lung parenchyma. Histologically, the nodules consist of an outer lamellated fibrous capsule enclosing hyalinized collagen or necrotic tissue. Scattered small calcifications of varying sizes (1–10 mm) can be seen (24).

Although the pattern of most viral pneumonia exhibits similarity on the basis of viridae, there are some exceptions for varicellovirus, which shows a different pattern compared with HSV. Chest radiographic findings of varicella-zoster virus pneumonia consist of multiple 5–10-mm ill-defined nodules that may be confluent (Fig 4a). Hilar lymphadenopathy and pleural effusion

are unusual but may also be present. After the improvement of the skin lesions, the small lung nodules typically disappear within a week but may persist for several weeks.

CT usually shows 1–10-mm well-defined or ill-defined nodules with a surrounding halo of GGO, patchy GGO, and coalescence of nodules diffusely throughout both lungs. The lesions may calcify, and well-defined scattered 2–3-mm hyperattenuating calcifications can persist (25). These small calcified nodules also can be seen in patients with other diseases such as pulmonary tuberculosis or pneumoconiosis, but in patients with varicella infections, these calcifications are usually tiny (2–3 mm), numerous, well defined, and randomly distributed rather than centrilobular or show perilymphatic distribution in otherwise normal lungs without definite fibrotic changes or other parenchymal abnormalities. In patients undergoing lung transplantation, mediastinal lymphadenopathy and interlobular septal thickening have been reported (26). These findings also disappear with healing of the skin lesions after antiviral therapy (24). In patients with active chickenpox, predisposing factors, and new pulmonary infiltrates with small nodules,

Figure 3. Pneumonia due to HSV in a 72-year-old woman with multiple myeloma. **(a)** Initial chest radiograph shows ill-defined diffuse reticular areas of increased opacity (arrows) in both lungs. **(b, c)** Axial thin-section (1-mm collimation) CT images at the carina **(b)** and the left inferior pulmonary vein level **(c)** show diffuse interstitial and interlobular septal thickening (arrowheads) with patchy GGO (arrows) in both lungs. A small amount of bilateral pleural effusion (*) is noted.



the diagnosis of varicella-zoster virus pneumonia should be considered and/or excluded.

CMV (β Herpesvirinae)

CMV is a common human pathogen that usually causes an asymptomatic infection or mild flu-like symptoms in immunocompetent patients. However, it can cause life-threatening pulmonary infection in immunocompromised patients owing to reactivation of the latent virus or infusion of CMV-seropositive marrow or blood products. Transplantation and long-term corticosteroid therapy are important risk factors. Early (30–100 days) after transplantation is the critical time for CMV infection, and CMV infection is a frequent complication of both hematopoietic stem cell transplantation and solid-organ transplantation. For solid-organ transplantation, recipients of lung and small intestine transplants are at highest risk, and this may be associated with the intensity of immunosuppression and the amount of lymphoid tissue in transplanted organs.

The host factors can affect the pathophysiology of CMV infection. In patients who have received transplants, a T-cell-mediated response to infection induces antigens expressed in the lungs, resulting in

severe necrotizing pneumonia. However, in patients with AIDS, who have a more profound immune deficiency, it may be difficult to mount a serious immune response, and lung damage appears to be the direct result of the cytopathogenic effects of CMV, with a high density of CMV inclusion bodies and more severe and diffuse alveolar damage observed at histopathologic examination (27).

The predominant radiologic findings are bilateral asymmetric GGO, poorly defined small centrilobular nodules, and airspace consolidation (27) (Fig 5). Thickened interlobular septa also are observed. However, masses and masslike infiltrates can be more common in patients with AIDS than in non-AIDS patients (28,29). During the early period, up to 100 days after bone marrow transplantation, the two most common pathogens are CMV and angioinvasive aspergillosis. *Pneumocystis jirovecii* also can occur in the early periods after bone marrow transplantation, but because of effective prophylaxis with sulfamethoxazole/trimethoprim, it is now relatively rare in transplant recipients. The differentiation between pneumonia due to CMV or *Pneumocystis* is difficult, especially in the early phase of the disease, when bilateral GGO is seen on CT images. However, small

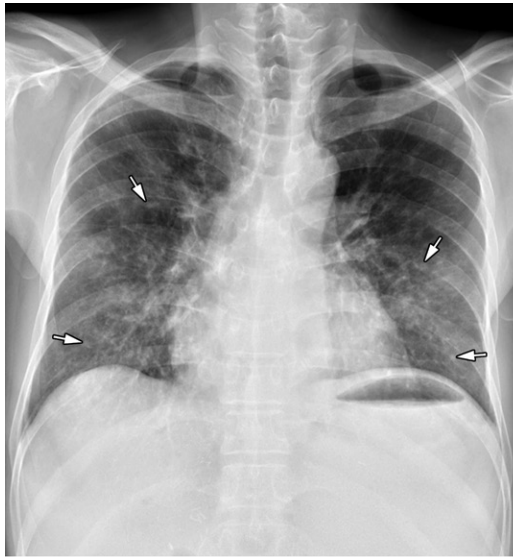
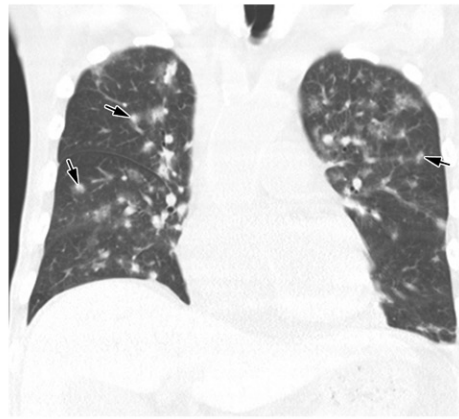


Figure 4. Pneumonia due to varicella-zoster virus (α Herpesvirinae) in a 53-year-old man who underwent liver transplantation 5 months before contracting the disease. **(a)** Initial chest radiograph shows multifocal reticulonodular infiltrations (arrows) in both lungs. **(b, c)** Thin-section (1-mm collimation) axial CT image **(b)** and coronal reconstructed CT image (5-mm thickness) **(c)** obtained on the same day show multifocal ill-defined small areas of nodular opacity (arrows) with the GGO halo sign in both lungs.

a.



b.



c.

nodules or ill-defined GGO and consolidation are typical features of CMV pneumonia, whereas apical distribution and homogeneous GGO are more frequently noted in patients with *Pneumocystis carinii* pneumonia (29).

Epstein-Barr Virus (γ Herpesvirinae)

Epstein-Barr virus infects B lymphocytes and pharyngeal epithelial cells. It is spread by means of direct person-to-person contact between susceptible individuals and those who are asymptomatic Epstein-Barr virus shedders. Infectious mononucleosis caused by Epstein-Barr virus infection usually occurs in adolescents with a triad of symptoms including fever with insidious onset of weakness (malaise), tonsillar pharyngitis, and lymphadenopathy. It resolves within several weeks or months without sequelae but may be accompanied by neurologic, hematologic, hepatic, respiratory, or psychological complications (30).

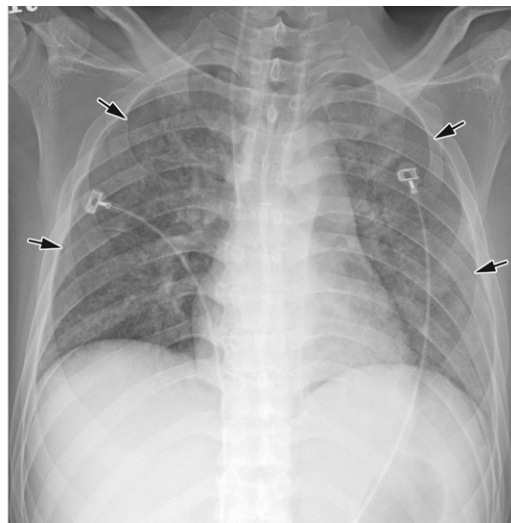
Intrathoracic involvement of infectious mononucleosis is very uncommon. The role of Epstein-Barr virus as an infective pathogen in

the development of lung disease is controversial. Rapidly progressive respiratory illness in patients with infectious mononucleosis rarely has been reported (31). Mononuclear inflammatory cells are apparent along bronchovascular bundles and interlobular septa in the interstitial pulmonary infiltrate at pathologic examination. These mononuclear cells are also present in the alveolar exudates (32). The most common radiologic abnormalities are mediastinal lymphadenopathy, and, rarely, interstitial infiltrates and widespread GGO can be seen. Splenomegaly is common. There are various types of lymphoproliferative disorders associated with Epstein-Barr virus infection, such as lymphomatoid granulomatosis, lymphoma, and posttransplantation lymphoproliferative disorder (31).

Parvoviridae

Bocavirus is a single-stranded DNA virus and a member of the family Parvoviridae, first isolated in 2005 from nasopharyngeal aspirate specimens from children (33). The virus is commonly

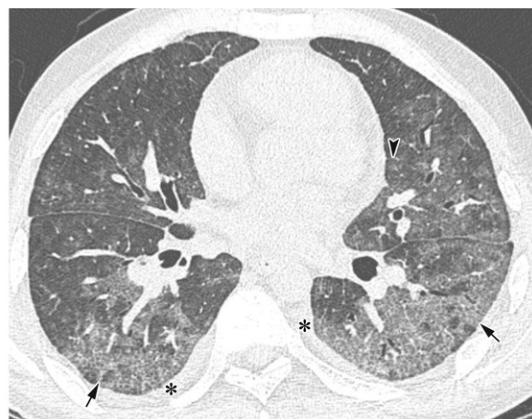
Figure 5. Pneumonia due to CMV in a 28-year-old man with graft-versus-host disease after bone marrow transplantation for chronic myeloblastic leukemia. (a) Initial chest radiograph shows diffuse ill-defined GGO (arrows) in both lungs. (b, c) Axial thin-section (1-mm collimation) CT images obtained on the same day, at the lower trachea level (b) and interlobar area level (c), show ill-defined GGO nodules, interlobular septal thickening (arrowheads), and diffuse GGO (arrows) in both lungs, with a scanty amount of bilateral pleural effusion (* in c).



a.



b.



c.

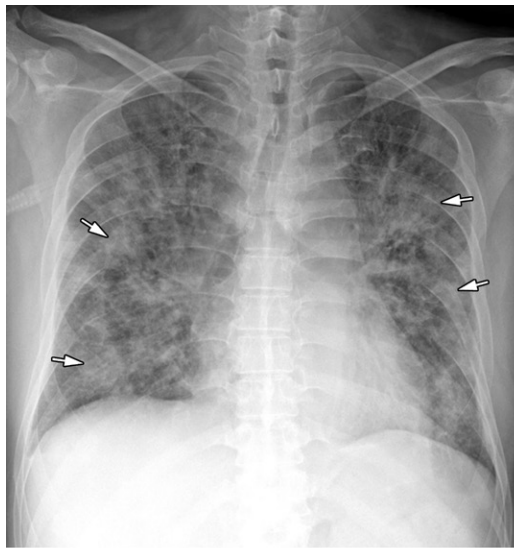
detected in nasopharyngeal aspirates of children who are suspected to have respiratory tract infections, and multiple viral coinfections are common (34). A recent prospective study of hospitalized children showed that human bocavirus is the fourth most commonly detected virus, with an incidence of 9.9%, followed by RSV (39.8%), rhinovirus (30.6%), and adenovirus (15%); 75% of bocavirus infections are coinfections with other viruses (35). Human bocavirus also is detected frequently in adults with mild respiratory symptoms. This virus may be associated with a spectrum of severity from a mild common cold, bronchiolitis, bronchopneumonia, or exacerbation of asthma to severe respiratory tract infection or bocavirus in combination with encephalitis (36,37). This pathogen contributes to severe pneumonia in immunocompromised adults (38). Although authors of some case reports have discussed the imaging findings of human bocavirus pneumonia as reticulonodular infiltration predominantly in both lower lobes (38), this virus is a recently discovered pathogen, and the imaging findings have not been well established. In our case (Fig 6),

human bocavirus infection manifested as diffuse bilateral patchy consolidation and GGO at chest radiography and patchy consolidation along the bronchovascular bundles with interlobular septal thickening at CT.

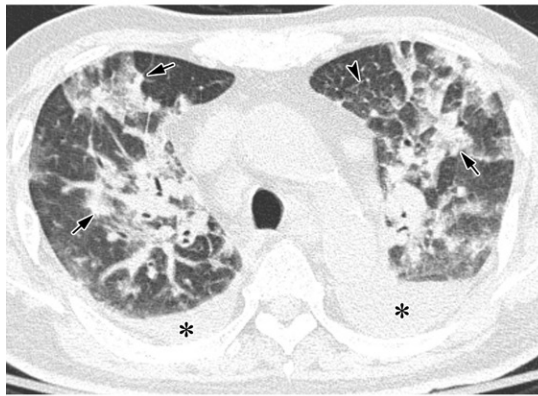
Paramyxoviridae

HPIV

HPIV is a single-stranded RNA virus and a member of the family Paramyxoviridae. HPIVs consist of four serotypes that cause respiratory illness by binding to the ciliated epithelium of the respiratory tract. The manifestations of HPIV infection are diverse, including otitis media, conjunctivitis, pharyngitis, croup, bronchitis, and pneumonia. HPIV infection is a common cause of disease and death in recipients of hematopoietic stem cell transplants and patients with hematologic malignancy (39). In hematopoietic stem cell transplant recipients, HPIV pneumonia exhibits 50% mortality during early stages and 75% 6-month mortality. HPIV is the second most commonly identified virus (20.8%) in patients admitted to



a.



b.



c.

Figure 6. Pneumonia due to human bocavirus in a 63-year-old man who presented with fever and had undergone chemotherapy for primary central nervous system lymphoma. (a) Chest radiograph shows diffuse irregular patchy consolidation (arrows) and GGO in both lungs. (b, c) Axial thin-section (1-mm collimation) chest CT images obtained on the same day show irregular patchy consolidation (arrows) along the bronchovascular bundles and in peripheral areas of the lungs, bronchial wall thickening, and interlobular septal thickening (arrowhead), with a small amount of bilateral pleural effusion (*).

the intensive care unit, and bacterial coinfection is common (40). This infection occurs predominantly (46.7%) from June to September.

At CT, HPIV pneumonia shows multifocal patchy consolidation with GGO that hinders differentiation of viral from bacterial pneumonia, and approximately one-fourth of patients show centrilobular nodules with bronchial wall thickening (41) (Fig 7).

Measles

Measles virus is a cause of childhood infections. Before the development of the measles vaccine, many people with measles presented with fever, maculopapular skin rash, cough, coryza, or conjunctivitis. Severe forms of measles include pneumonia, blindness, gastroenteritis, and encephalitis. Although global vaccination is being performed, measles remains a cause of death in children (42), and outbreaks are frequently reported, even in adults (43). Serious complications are reported, especially in pregnant women and immunocompromised patients, and mortality is high in immunocompromised patients (44,45).

Hilar lymphadenopathy and pleural effusion are commonly associated with measles (27). Typical measles pneumonia shows peribronchial nodular infiltration and reticulonodular infiltration with thickened interlobular septa; fibrosis may be seen on follow-up CT images (45).

Pneumoviridae

RSV Infection

Human RSV infection leads to bronchiolitis, pneumonia, and asthma in all age groups; infants, young children, and immunocompromised hosts are likely to present with severe respiratory infection (46). A recent prospective study (47) showed that RSV was the most common viral pathogen (28%) in children hospitalized for community-acquired pneumonia in the United States. In the study, children younger than 5 years were more prone to infection than were older children (37% vs 8%, respectively). RSV infection was noted to be common in adults who require admission to an intensive care unit from November to February (40).

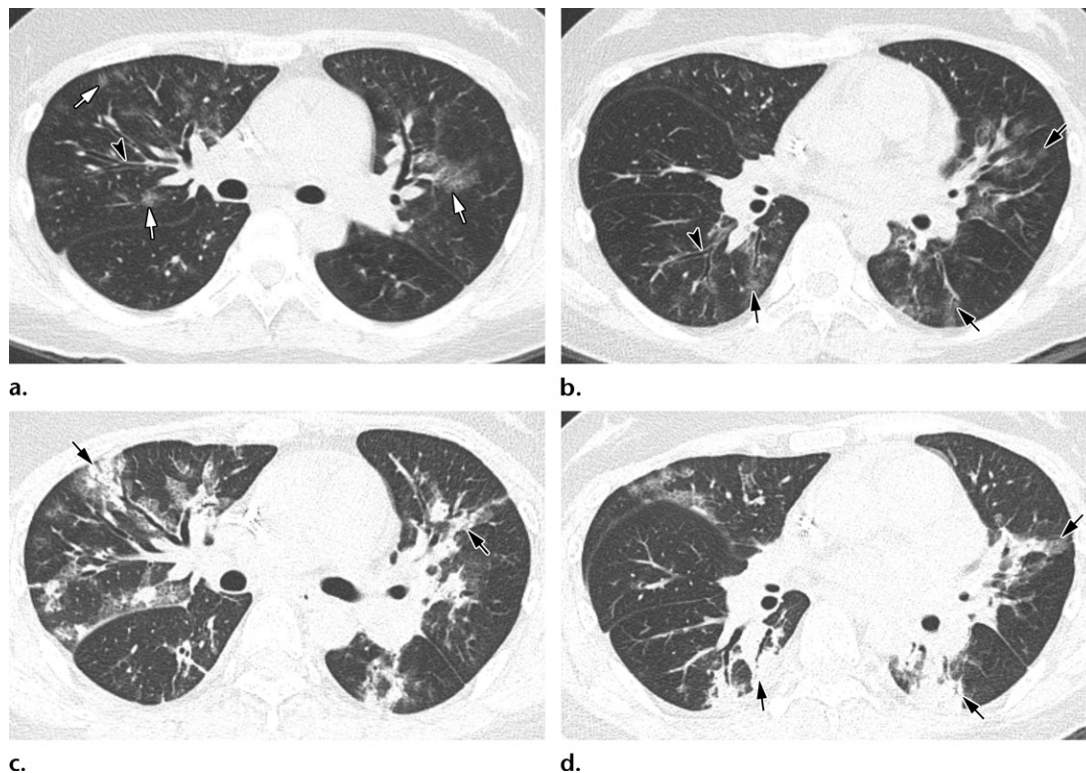


Figure 7. Pneumonia due to HPIV in a 22-year-old woman who presented with fever and had undergone haploidentical bone marrow transplantation for acute lymphoblastic leukemia 1 month before infection. (a, b) Initial axial chest CT images at the main bronchial level (a) and the interlobar area level (b) show multifocal ill-defined nodular GGO lesions (arrows) along the bronchovascular bundles and mild bronchial wall thickening (arrowheads). Prolonged neutropenia is noted. (c, d) Follow-up axial chest CT images obtained 10 days later show an increased extent and intensity of lesions and increased irregular consolidation (arrows) along the bronchovascular bundles. The patient died despite intensive medical care.

CT could provide clues to differentiating among pathogens that cause viral pneumonia on the basis of imaging patterns, especially RSV and adenovirus infections (2). RSV shows an airway-centric distribution, with areas of tree-in-bud opacity and bronchial wall thickening, with or without consolidation along the bronchovascular bundles (Fig 8).

HMPV Infection

HMPV was first identified in 2001; the structure of the virus is similar to that of RSV, and this virus can cause upper and lower respiratory tract infection. HMPV pneumonia accounts for 4% of community-acquired pneumonia in immunocompetent adults and is prevalent during winter months. Immunocompetent patients usually recover without risk of death (48). In comparison, HMPV infection causes severe pneumonia with mortality of 10%–40% in hematopoietic stem cell transplant recipients, with a 5% incidence of infection. Approximately 60% of hematopoietic stem cell transplantation recipients with HMPV infection progress to pneumonia; the risk factors of progression to pneumonia are systemic high-dose corticosteroid use and low lymphocyte counts (49).

Radiographs in patients with HMPV pneumonia show multilobar infiltrations (48). CT findings in immunocompetent patients with HMPV pneumonia have not been described yet; however, bilateral ill-defined centrilobular nodules, branching centrilobular nodules, and GGO are noted in patients with hematologic malignancy (50) (Fig 9). Pleural effusion is not common.

Bunyaviridae

Until recently, Bunyaviridae was the largest group of RNA viruses, but it was replaced by Hantaviridae and Phenuiviridae. Hantaviruses are transmitted by rodent vectors, while the others in Bunyaviridae are transmitted by arthropod vectors. Many types of Bunyaviruses can cause febrile infections, including hemorrhagic fever and encephalitis, in humans (51).

Severe Fever with Thrombocytopenia Syndrome Virus

Severe fever with thrombocytopenia syndrome virus is a type of tick-borne Phlebovirus. The virus was first isolated from the Hubei and Henan provinces in central China in 2010 and has since been reported in South Korea and Japan, mostly

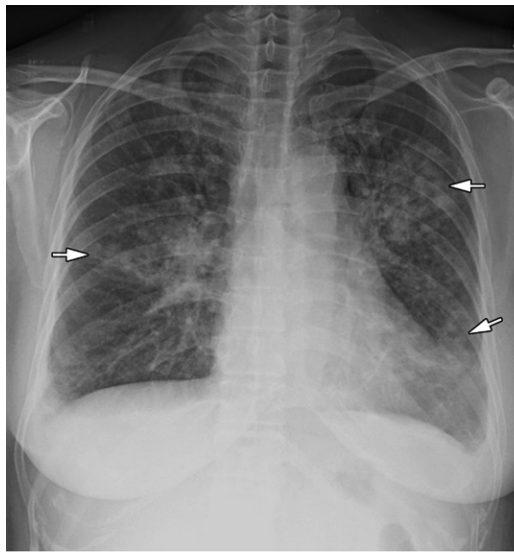
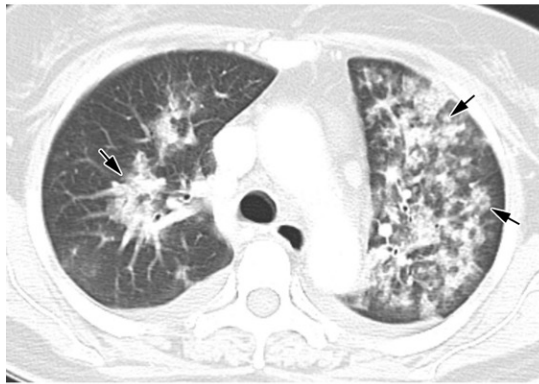
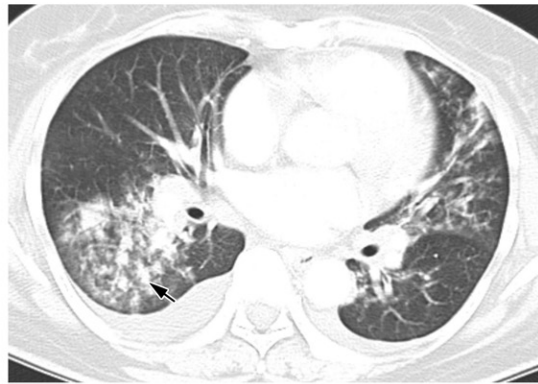


Figure 8. Pneumonia due to RSV in a 58-year-old woman with acute myeloid leukemia who presented with fever. (a) Initial chest radiograph shows multiple irregular nodular peribronchial air spaces or GGO (arrows) in both lungs and a small amount of bilateral pleural effusion. (b, c) Axial chest CT images obtained on the same day at the lower trachea level (b) and the interlobar area level (c) show multiple irregular areas of nodular tree-in-bud opacity and patchy consolidations (arrows) along the bronchovascular bundles and mild bronchial wall thickening.

a.



b.



c.

arising as sporadic cases in the spring and summer (52–54). Farmers and those who work in the field are the major at-risk group. Outdoor activity such as hiking and camping also is a potential risk factor for tick exposure. Direct contact with infected blood also can cause infection (51). Clinical symptoms include fever, gastrointestinal problems, myalgia, thrombocytopenia, and increased liver enzyme levels. Severe fever with thrombocytopenia syndrome must be differentiated from hemorrhagic fever with renal syndrome or leptospirosis (52). The initial chest radiograph may be normal, but several days later, bilateral pulmonary infiltration indicating pulmonary edema develops (55). Pleural effusion is common.

Hantavirus

Hantavirus is another genus of Bunyaviridae; its member viruses exist in the environment because of persistent infection of their hosts, typically rodents, insectivores, and bats. More than 40 hantavirus species are known, and greater than 20 of these are considered pathogenic in humans. Annually, more than 20 000 cases of hantavirus in-

fection are reported globally, the majority of which occur in Asia, but increasing numbers are reported in the Americas and Europe (56,57). Humans can contract a hantavirus infection by inhaling air contaminated with the virus concealed in the excreta, saliva, or urine of infected animals. Pathogenic hantavirus is one of the few viral pathogens that target endothelial cells throughout the body, with two different clinical manifestations that usually are related to the kidney (hemorrhagic fever with renal syndrome) or lung (hantavirus cardiopulmonary syndrome). The morbidity of hemorrhagic fever with renal syndrome is 1%–15%. Hantavirus cardiopulmonary syndrome is much more lethal, with morbidity of 40%–50% (58).

Hantavirus cardiopulmonary syndrome characteristically involves the lung and manifests as respiratory distress from noncardiogenic edema. After a 17–42-day incubation period, clinical phases initiate with the prodromal phase and continue to cardiopulmonary and convalescent phases. Clinical symptoms include dry cough and rapidly increasing dyspnea (57). Radiologic findings are usually normal initially or consist of minimal

Figure 9. Pneumonia due to HMPV in a 50-year-old woman who presented with fever, cough, and sputum. (a) Initial chest radiograph shows multinodular airspace opacity (arrows) in the right lung. (b, c) Thin-section (1-mm collimation) axial (b) and coronal (c) reconstructed (5-mm section thickness) chest CT images obtained on the same day show multiple ill-defined centrilobular nodules (arrows) or GGO (arrowheads) along the bronchovascular bundles and mild bronchial wall thickening in both lungs, especially in the right lung.



a.

c.



b.

interstitial edema. Pleural effusion is common (Fig 10). Pulmonary interstitial edema can be striking, although it usually is transient. In some cases, the findings rapidly progress to bilateral airspace consolidation and fulminant respiratory deterioration within 48 hours. These pulmonary findings are occasionally secondary to renal failure (59).

Orthomyxoviridae

Influenza A, B, and C

Influenza viruses are members of the Orthomyxoviridae family. They are single-stranded RNA viruses that are divided into three groups (A, B, and C) according to internal membrane and nucleoprotein antigens. Of these three groups, type A and occasionally type B organisms cause influenza virus pneumonia. Influenza virus is an important pathogen that causes seasonal upper respiratory tract infections, including those of the trachea and major bronchi, which cause periodic, endemic, and pandemic infections. Infections are usually mild and restricted to the upper respiratory tract. However, in individuals with chronic diseases, the elderly, and infants, severe complications from influenza A viruses, including hemorrhagic bronchitis or fulminant pneumonia (primary viral or secondary bacterial), may occur. Infections usually occur as annual winter outbreaks; however, pandemic influenza viruses occasionally arise. Influenza A virus can be classified into subtypes on the basis of two surface proteins of the virus, which are the hemagglutinin and the neuraminidase, or H

and N. Swine influenza caused by influenza type A virus includes subtypes H1N1, H1N2, H2N1, H3N1, H3N2, and H2N3. An H1N1 pandemic reported in more than 70 countries with 30 000 cases of infection occurred in 2009 (60).

Influenza virus replicates in the respiratory epithelial cells, and replication peaks approximately 48 hours after inoculation into the nasopharynx. The early stages of disease often demonstrate tracheobronchitis and neutrophilic bronchopneumonia. The airway walls are congested, and mononuclear cell infiltrates and degeneration of epithelial cells are noted. In the later stage, parenchymal change shows typical features of diffuse alveolar damage, with intra-alveolar edema and hemorrhage (61,62).

Radiographs in patients with influenza pneumonia show bilateral reticulonodular areas of opacity with or without focal areas of consolidation, usually in the lower lobes. Poorly defined patchy or nodular areas of consolidation that

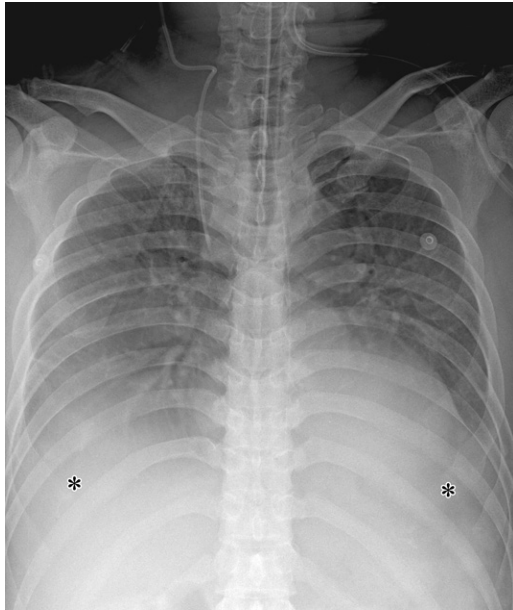


Figure 10. Hantavirus in a 52-year-old man who presented with fever and acute renal failure. Initial chest CT findings were normal (not shown). Chest radiograph obtained 1 day after presentation, when the patient suddenly progressed to having decreased blood pressure, shows pulmonary edema and bilateral pleural effusion (*). The test result for hantavirus antibodies was positive, and the titer was increased to 1:512. Intensive medical treatment was performed and the patient recovered.

become rapidly confluent and represent either diffuse alveolar damage or superinfection are seen frequently and resolve in 3 weeks (63) (Fig 11). Bilateral patchy consolidation, ill-defined small nodules, and patchy GGOs associated with the areas of consolidation have been reported in patients with underlying hematologic malignancy (64). However, similar findings have been reported in healthy hosts during the H1N1 epidemic (65). Patients who progress to having more diffuse lung damage can demonstrate findings of acute respiratory distress syndrome or, in cases of H1N1, organizing pneumonia (66). Pleural effusion is rare. Secondary bacterial pneumonia can occur; *Streptococcus pneumoniae* infection, in particular, has an important interaction, and coinfection or secondary infection may exist. Superimposed bacterial infection can be suspected when secondary fever is noted after a period of defervescence, an increase in white blood cell count, and changes in radiologic abnormality. Lobular consolidation can be especially helpful in diagnosis of bacterial-superimposed infection (67). Gram stain and culture of sputum or bronchoalveolar lavage also are helpful methods to confirm the superimposed bacterial infection when it is suspected.

Avian flu is caused by the H5N1 subtype of influenza type A, and most human infection occurs after close contact with infected birds. Overall

mortality for influenza A (H5N1) is as high as 60%, and there have been outbreaks in Hong Kong. The most common imaging finding of Avian flu is multifocal consolidation. Reported CT findings include focal, multifocal, or diffuse GGO and areas of consolidation. Centrilobular nodules, pseudocavitation, pneumatocele formation, and lymphadenopathy also are seen often (68). During the course of disease, pleural effusions and cavitation also can develop. Patients usually present with a rapidly progressive pneumonia that results in acute respiratory distress syndrome.

Coronaviridae

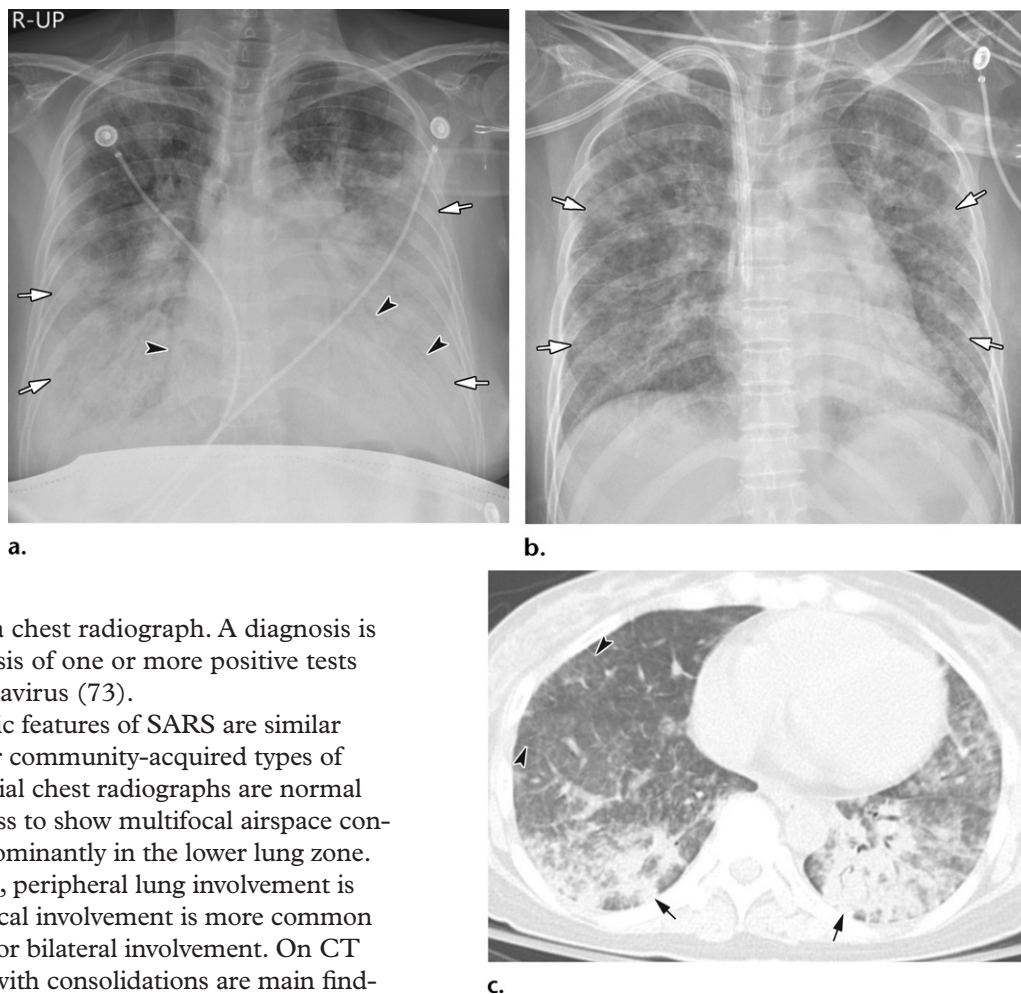
Human coronaviruses are considered as important pathogens that cause infections in pediatric, geriatric, and immunocompromised patients and include upper and lower respiratory tract infections (pneumonia and bronchiolitis) and even acute respiratory distress syndrome (69). SARS coronavirus was identified as a member of the family Coronaviridae in late 2003 after a world-wide epidemic. In 2012, another coronavirus-related epidemic occurred in the Middle East that was identified as MERS (70). Angiotensin-converting enzyme 2 is a potential SARS virus receptor and is a negative regulator of the renin-angiotensin system that affects vascular permeability (71). Angiotensin-converting enzyme 2 is expressed in the lungs and kidneys, and the SARS virus induces direct lung injury by involving angiotensin-converting enzyme, which contributes to diffuse alveolar damage. Also, SARS coronavirus-encoded proteins induce cell apoptosis, including that of the lungs, kidneys, and liver. MERS coronavirus can evade immune response and cause a severe dysregulation of the host cellular transcriptome, resulting in apoptosis of cells (72).

SARS Coronavirus

A worldwide outbreak of SARS coronavirus, which was first identified in Guangdong Province, China, occurred during 2002–2003. There were more than 8000 cases of identified infection, with 21% occurring in health care workers. SARS mortality in 2003 was estimated at 6.8%–13.2% for patients younger than 60 years and 43%–50% for patients older than 60 years. Patients with comorbidities such as diabetes or chronic hepatitis exhibited increased mortality. The animal hosts of SARS coronavirus appear to include the masked palm civet, raccoon dogs, and the Chinese ferret-badger (73).

After a 2–10-day incubation period, patients present with flu-like symptoms, dyspnea, and recurrent or persistent fever. Patients typically have a history of exposure and new infiltration of

Figure 11. Pneumonia due to influenza A virus in a 38-year-old pregnant woman at the gestational age of 29 weeks and 5 days who presented with a cough and dyspnea. **(a)** Initial chest radiograph shows extensive patchy consolidation (arrows) with air bronchogram (arrowheads) in both lungs, especially in the middle to lower lung zones. After the patient underwent an emergency cesarean delivery, intubation and extracorporeal membrane oxygenation were performed for acute respiratory distress syndrome. **(b)** Chest radiograph obtained 3 weeks later shows decreased intensity of irregular consolidation (arrows). **(c)** Axial CT image obtained on the same day as **b** shows irregular consolidation (arrows) along the bronchovascular bundles and diffuse GGO with interlobular septal thickening (arrowheads) in both lungs. The patient underwent reverse-transcription polymerase chain reaction for viral infection with sputum and blood culture and bronchoalveolar lavage to find superimposed infection. However, there was no evidence of coinfection.



pneumonia on a chest radiograph. A diagnosis is made on the basis of one or more positive tests for SARS coronavirus (73).

The radiologic features of SARS are similar to those of other community-acquired types of pneumonia. Initial chest radiographs are normal but soon progress to show multifocal airspace consolidation, predominantly in the lower lung zone. In most patients, peripheral lung involvement is common. Unifocal involvement is more common than multifocal or bilateral involvement. On CT images, GGOs with consolidations are main findings, and reticulation is noted after the 2nd week (74). Cavitation, lymphadenopathy, or pleural effusions are not common findings (75).

MERS Coronavirus

MERS coronavirus is a new member of the β -coronaviruses and is different from SARS and other endemic human β -coronaviruses (eg, OC43, HKU1). The first case was identified in September 2012, in Riyadh, Saudi Arabia. Bats and dromedary camels are considered to be reservoirs of MERS coronavirus. The virus was named SARS-like coronavirus, novel coronavirus, or human coronavirus Erasmus Medical Center (EMC) when it was first discovered. During 2012–2014, the number of cases of MERS coronavirus infection increased in Saudi Arabia, with overall mortality of 35%–44% (76). MERS was reported in at least 10 other countries in Europe and Asia and in the United States and

was associated with travel to the Middle East (77). In May 2015, a large outbreak of MERS coronavirus infection occurred in South Korea, with 186 identified patients and 38 deaths.

Clinical symptoms resemble other lower respiratory tract diseases involving fever, cough, dyspnea, and pneumonia. The infection may progress rapidly to acute respiratory distress syndrome, multiorgan failure, and death. MERS progresses more rapidly to respiratory failure than does SARS and induces acute kidney injury. Approximately 20% of all virus cases were identified in health care workers and persons who come into close contact with camels (76).

MERS pneumonia appears on CT images as subpleural and basilar airspace lesions, with extensive GGO and consolidation (78) (Fig 12).

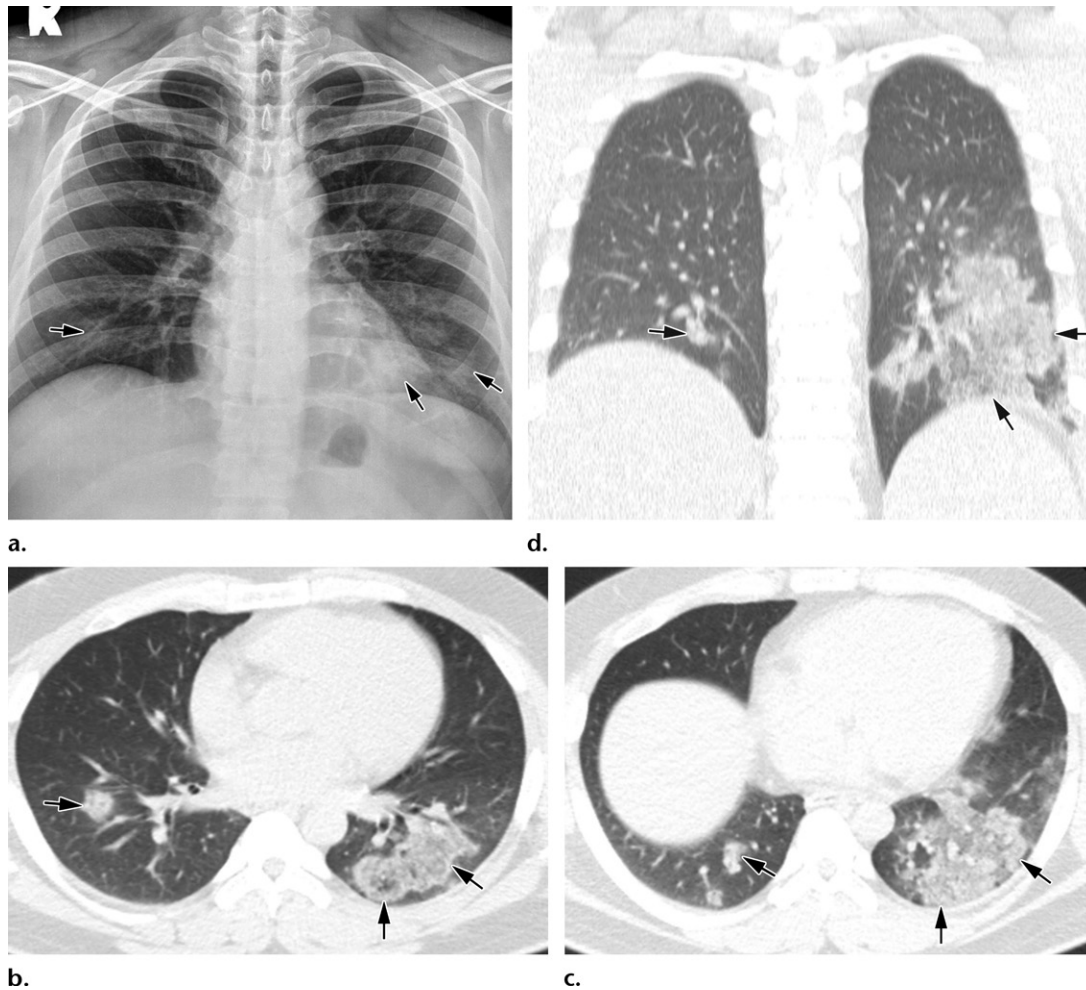


Figure 12. Pneumonia due to MERS coronavirus in a 27-year-old man who presented with a cough and sputum. (a) Initial chest radiograph shows increased areas of ill-defined nodular opacity (arrows) in both lower lung zones, especially in the left retrocardiac area. (b–d) Axial CT images (3-mm section thickness) obtained on the same day at the level of the right inferior pulmonary vein (b) and the junction of the right atrium and inferior vena cava (c) and a coronal reconstruction image at the vertebral body level (d) show multifocal patchy and nodular consolidation with GGO (arrows) in both lower lobes.

Cavitation is uncommon. In a patient with a history of close contact with a MERS coronavirus patient, lymphopenia with early manifestation of peripheral GGO on a chest radiograph might be suspected to be a MERS coronavirus infection (79). Pleural effusion and pneumothorax are more common in patients who died than in those who recovered (79). After recovery, these abnormalities show marked improvement, but fibrotic changes remain (80).

Picornaviridae

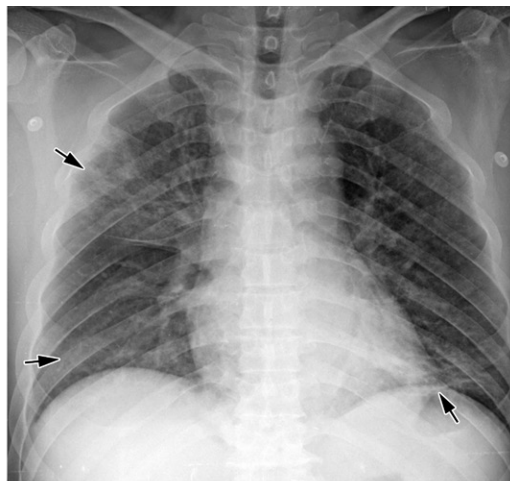
Rhinovirus A, B, and C

Human rhinovirus is a major pathogen of respiratory infection detected in 18%–26% of pediatric patients and in 2%–17% of adult patients with community-acquired infectious pneumonia (81,82). Rhinovirus is the predominant cause of the common cold during all four seasons but more frequently is detected in spring and au-

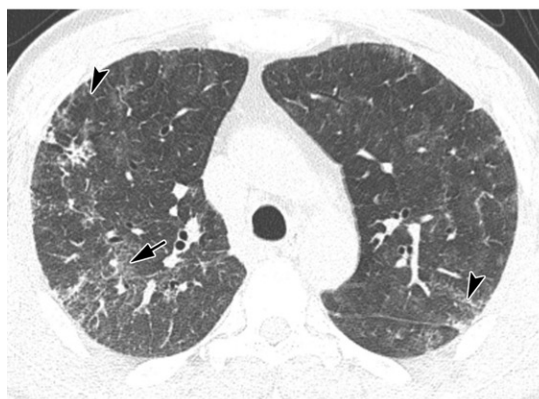
turn. The incidence of severe pneumonia does not differ among human rhinovirus A (18.6%), human rhinovirus B (21.4%), and human rhinovirus C (20.0%), and in-hospital mortality rates also do not differ significantly (81). Bacterial coinfection is not common (18.5%) and less than that with influenza (83). Immunocompromised patients are more prone to infection. Rhinovirus has no cytopathic effect on the respiratory epithelium; however, it can cause disruption of the epithelial barrier, which leads to increased vascular permeability and mucous secretion (84).

In patients with severe pneumonia who require admission to the intensive care unit, human rhinovirus was the most commonly identified viral pathogen (40). In patients with severe rhinovirus pneumonia, bilateral patchy consolidation with multifocal GGO and interlobular septal thickening are noted (83) (Fig 13).

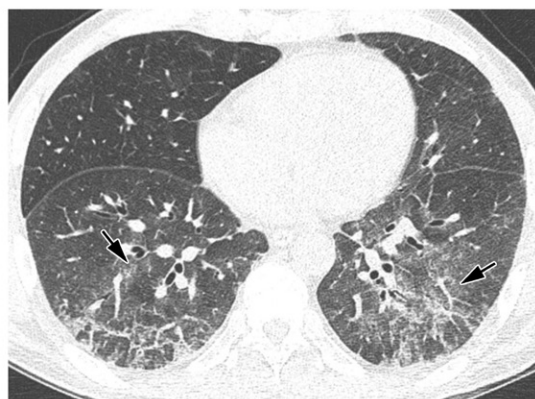
Figure 13. Pneumonia due to rhinovirus in a 51-year-old man with acute myeloid leukemia who presented with dyspnea 3 months after bone marrow transplantation. (a) Initial chest radiograph shows irregular ill-defined patchy increased opacity (arrows) in both lungs. (b, c) Axial CT images obtained on the same day at the lower trachea level (b) and both lower lobe basal segments (c) show irregular areas of increased opacity with interlobular septal thickening (arrowheads) and ill-defined patchy GGO (arrows) in both lungs.



a.



b.



c.

Antiviral Treatment

Several antiviral drugs are currently available (Table 3). Antiherpes drugs inhibit viral replication by acting as competitive substrates for viral DNA polymerase. Influenza virus drugs inhibit the ion channel M2 protein or the enzyme neuraminidase. Ribavirin is multipotent for the treatment of RSV, adenovirus, HPIV, and HMPV. Cidofovir also can be used for the treatment of CMV, herpesviruses, drug-resistant varicella-zoster virus, and Epstein-Barr virus (85,86). Antiviral therapy can reduce attack rates and decrease outbreaks and could reduce the public health burden. For example, the use of antiviral therapy for influenza is important in reducing the infection rate and preventing outbreaks (87). Recently, clarithromycin-naproxen-oseltamivir combination therapy for influenza A (H3N2) showed a reduction in mortality and length of hospital stay (88).

Conclusion

CT patterns of viral pneumonia are related to the pathogenesis of viral infections. Although not all patients present with typical patterns, most viral pneumonia imaging patterns share similarity on the basis of viridae, because viruses of the same

viridae have a similar pathogenesis. Although a definite diagnosis cannot be achieved by using imaging features alone, recognition of viral pneumonia patterns may help in the differentiation among viral pathogens and reduce the unnecessary use of antibiotics. Further studies aimed at elucidating the imaging findings of newly identified viral pathogens, including human bocavirus and coronaviruses, could be of value for proper diagnosis and improvement of clinical outcomes.

References

1. Pavia AT. Viral infections of the lower respiratory tract: old viruses, new viruses, and the role of diagnosis. *Clin Infect Dis* 2011;52(suppl 4):S284–S289.
2. Miller WT Jr, Mickus TJ, Barbosa E Jr, Mullin C, Van Deerlin VM, Shiley KT. CT of viral lower respiratory tract infections in adults: comparison among viral organisms and between viral and bacterial infections. *AJR Am J Roentgenol* 2011;197(5):1088–1095.
3. Kahn JS. Newly identified respiratory viruses. *Pediatr Infect Dis J* 2007;26(8):745–746.
4. Kahn JS. Newly discovered respiratory viruses: significance and implications. *Curr Opin Pharmacol* 2007;7(5):478–483.
5. Azhar EI, Lanini S, Ippolito G, Zumla A. The Middle East respiratory syndrome coronavirus: a continuing risk to global health security. *Adv Exp Med Biol* 2017;972:49–60.
6. Hall CB. Respiratory syncytial virus and parainfluenza virus. *N Engl J Med* 2001;344(25):1917–1928.
7. Chang A, Masante C, Buchholz UJ, Dutch RE. Human metapneumovirus (HMPV) binding and infection are mediated by

Table 3: Taxonomy of Viral Pneumonia Pathogens, Diagnostic Tests, and Treatment

Order (-virales)	Family (-viridae) and Subfamily [-virinae]	Genus (-virus)	Species (-virus)	Common Name	Diagnostic Test*	Treatment Option†
Adeno- Herpes-	Mastadeno-	Human mastadeno-	Adenovirus		NAT, antigen detection, culture	Cidofovir, IVIG
	Herpes-[Alphaherpes-]	Simplex-	Human alphaherpes- 1 and 2	HSV	NAT, antigen detection, Tzanck smear, serology	Acyclovir
Herpes- [Betaherpes-]	Varicello-	Human alphaherpes- 3	Varicella zoster virus		NAT, serology, culture	Acyclovir
	Cytomegalo-	Human betaherpes- 5	CMV		NAT, CMV antigenemia (blood), culture, serology	Ganciclovir, foscarnet, IVIG, CMV IG
Unassigned	Herpes- [Gammaherpes-]	Lymphocrypto-	Human gammaherpes- 4	Epstein-Barr virus	NAT, serology	Acyclovir
	Parvo-[Parvo-]	Bocaparvo-	Primate bocaparvo- 1 and 2	Bocavirus	NAT	No specific treatment
Mononega-	Paramyxo-	Respiro-	Human respiro- 1 and 3	HPIV	NAT, culture, antigen detection	Ribavirin, IVIG
		Morbilli-	Measles morbilli-	Measles	NAT, serology, culture, antigen detection	Ribavirin
Pneumo-	Rubula-	Mumps rubula-	Mumps		NAT, serology, culture	No specific treatment
	Orthopneumo-	Human orthopneumo-	RSV		NAT, antigen detection, culture	Ribavirin, IVIG
Bunya-	Hanta-	Metapneumo-	Human metapneumo-	HMPV	NAT, culture, antigen detection	Ribavirin
		Orthohanta-	Hantaan orthohanta-	Hantavirus cardiopulmonary syndromes, hemorrhagic fever with renal syndrome	NAT (blood), serology	No specific treatment
Unassigned	Phenui-	Phlebo-	Severe fever with thrombocytopenia syndrome phlebo-		NAT (blood), serology	No specific treatment
		Influenza-	Rift Valley fever phlebo-	Rift Valley fever	NAT (blood), serology	No specific treatment
Nido-	Corona-[Corona-]	Alphacorona-	Human corona-	Coronavirus	NAT, serology	No specific treatment
		Betacorona-	SARS-related MERS-related	SARS MERS	NAT, serology	No specific treatment
Picorna-	Entero-	Enterovirus	Rhino-Enterovirus	Rhinovirus Enterovirus	NAT, culture	Ribavirin, interferon α -2a
		Influenza-	Influenza-	Influenza	NAT, antigen detection, culture	No specific treatment

Note.—Viral order names end with “virales,” family names end with “viridae,” subfamily names end with “virinae,” genus names end with “virus,” and species names include the name of the disease with “virus.” IG = immunoglobulin, IVIG = intravenous immunoglobulin, NAT = nucleic acid amplification test.

*Specimens for diagnostic test were respiratory samples (nasopharyngeal swab or aspirate, sputum, tracheal aspirate, or bronchoalveolar lavage fluid), unless otherwise stated.

†In immunocompromised patients, the reduction of immunosuppressive drugs generally is recommended.

- interactions between the HMPV fusion protein and heparan sulfate. *J Virol* 2012;86(6):3230–3243.
8. Franquet T. Imaging of pulmonary viral pneumonia. *Radiology* 2011;260(1):18–39.
 9. Chong S, Kim TS, Cho EY. Herpes simplex virus pneumonia: high-resolution CT findings. *Br J Radiol* 2010;83(991):585–589.
 10. Podlech J, Holtappels R, Pahl-Seibert MF, Steffens HP, Reddehase MJ. Murine model of interstitial cytomegalovirus pneumonia in syngeneic bone marrow transplantation: persistence of protective pulmonary CD8-T-cell infiltrates after clearance of acute infection. *J Virol* 2000;74(16):7496–7507.
 11. Buckwalter SP, Teo R, Espy MJ, Sloan LM, Smith TF, Pritt BS. Real-time qualitative PCR for 57 human adenovirus types from multiple specimen sources. *J Clin Microbiol* 2012;50(3):766–771.
 12. Yoon H, Jhun BW, Kim SJ, Kim K. Clinical characteristics and factors predicting respiratory failure in adenovirus pneumonia. *Respirology* 2016;21(7):1243–1250.
 13. Lewis PF, Schmidt MA, Lu X, et al. A community-based outbreak of severe respiratory illness caused by human adenovirus serotype 14. *J Infect Dis* 2009;199(10):1427–1434.
 14. Park JY, Kim BJ, Lee EJ, et al. Clinical features and courses of adenovirus pneumonia in healthy young adults during an outbreak among Korean military personnel. *PLoS One* 2017;12(1):e0170592.
 15. Hubmann M, Fritsch S, Zoellner AK, et al. Occurrence, risk factors and outcome of adenovirus infection in adult recipients of allogeneic hematopoietic stem cell transplantation. *J Clin Virol* 2016;82:33–40.
 16. Aquino SL, Dunagan DP, Chiles C, Haponik EF. Herpes simplex virus 1 pneumonia: patterns on CT scans and conventional chest radiographs. *J Comput Assist Tomogr* 1998;22(5):795–800.
 17. Gasparetto EL, Escuissato DL, Inoue C, Marchiori E, Müller NL. Herpes simplex virus type 2 pneumonia after bone marrow transplantation: high-resolution CT findings in 3 patients. *J Thorac Imaging* 2005;20(2):71–73.
 18. Graham BS, Snell JD Jr. Herpes simplex virus infection of the adult lower respiratory tract. *Medicine (Baltimore)* 1983;62(6):384–393.
 19. Byers RJ, Hasleton PS, Quigley A, et al. Pulmonary herpes simplex in burns patients. *Eur Respir J* 1996;9(11):2313–2317.
 20. Ramsey PG, Fife KH, Hackman RC, Meyers JD, Corey L. Herpes simplex virus pneumonia: clinical, virologic, and pathologic features in 20 patients. *Ann Intern Med* 1982;97(6):813–820.
 21. Travis WD, Colby TV, Koss MN, Rosado-de-Christenson ML, Muller NL, TE K. Non-neoplastic disorders of the lower respiratory tract. Washington, DC: American Registry of Pathology, 2002.
 22. Umans U, Golding RP, Duraku S, Manoliu RA. Herpes simplex virus 1 pneumonia: conventional chest radiograph pattern. *Eur Radiol* 2001;11(6):990–994.
 23. Alanezi M. Varicella pneumonia in adults: 13 years' experience with review of literature. *Ann Thorac Med* 2007;2(4):163–165.
 24. Kim JS, Ryu CW, Lee SI, Sung DW, Park CK. High-resolution CT findings of varicella-zoster pneumonia. *AJR Am J Roentgenol* 1999;172(1):113–116.
 25. Hughes DP, Lea S, Wahbi ZK. Varicella pneumonia. *EU-RORAD - Radiologic Teaching Files*, 2007.
 26. Maher TM, Gupta NK, Burke MM, Carby MR. CT findings of varicella pneumonia after lung transplantation. *AJR Am J Roentgenol* 2007;188(6):W557–W559.
 27. Kim EA, Lee KS, Primack SL, et al. Viral pneumonias in adults: radiologic and pathologic findings. *RadioGraphics* 2002;22(Spec No):S137–S149.
 28. McGuinness G, Scholes JV, Garay SM, Leitman BS, McCauley DI, Naidich DP. Cytomegalovirus pneumonitis: spectrum of parenchymal CT findings with pathologic correlation in 21 AIDS patients. *Radiology* 1994;192(2):451–459.
 29. Vogel MN, Brodoefel H, Hierl T, et al. Differences and similarities of cytomegalovirus and pneumocystis pneumonia in HIV-negative immunocompromised patients: thin section CT morphology in the early phase of the disease. *Br J Radiol* 2007;80(955):516–523.
 30. Jenson HB. Acute complications of Epstein-Barr virus infectious mononucleosis. *Curr Opin Pediatr* 2000;12(3):263–268.
 31. Miyake H, Matsumoto A, Komatsu E, et al. Infectious mononucleosis with pulmonary consolidation. *J Thorac Imaging* 1996;11(2):158–160.
 32. Myers JL, Peiper SC, Katzenstein AL. Pulmonary involvement in infectious mononucleosis: histopathologic features and detection of Epstein-Barr virus-related DNA sequences. *Mod Pathol* 1989;2(5):444–448.
 33. Allander T, Tammi MT, Eriksson M, Bjerkner A, Tiveljung-Lindell A, Andersson B. Cloning of a human parvovirus by molecular screening of respiratory tract samples. *Proc Natl Acad Sci U S A* 2005;102(36):12891–12896 [Published correction appears in *Proc Natl Acad Sci U S A* 2005;102(43):15712.].
 34. Christensen A, Nordbø SA, Krokstad S, Rognlien AG, Døllner H. Human bocavirus commonly involved in multiple viral airway infections. *J Clin Virol* 2008;41(1):34–37.
 35. Calvo C, García-García ML, Pozo F, Carballo D, Martínez-Monteserin E, Casas I. Infections and coinfections by respiratory human bocavirus during eight seasons in hospitalized children. *J Med Virol* 2016;88(12):2052–2058.
 36. Akturk H, Sik G, Salman N, et al. Atypical presentation of human bocavirus: severe respiratory tract infection complicated with encephalopathy. *J Med Virol* 2015;87(11):1831–1838.
 37. Allander T, Jartti T, Gupta S, et al. Human bocavirus and acute wheezing in children. *Clin Infect Dis* 2007;44(7):904–910.
 38. Kupfer B, Vehreschild J, Cornely O, et al. Severe pneumonia and human bocavirus in adult. *Emerg Infect Dis* 2006;12(10):1614–1616.
 39. Shah DP, Shah PK, Azzi JM, Chemaly RF. Parainfluenza virus infections in hematopoietic cell transplant recipients and hematologic malignancy patients: a systematic review. *Cancer Lett* 2016;370(2):358–364.
 40. Choi SH, Hong SB, Ko GB, et al. Viral infection in patients with severe pneumonia requiring intensive care unit admission. *Am J Respir Crit Care Med* 2012;186(4):325–332.
 41. Kim MC, Kim MY, Lee HJ, et al. CT findings in viral lower respiratory tract infections caused by parainfluenza virus, influenza virus and respiratory syncytial virus. *Medicine (Baltimore)* 2016;95(26):e4003.
 42. Rota PA, Moss WJ, Takeda M, de Swart RL, Thompson KM, Goodson JL. Measles. *Nat Rev Dis Primers* 2016;2:16049.
 43. Caseris M, Houhou N, Longuet P, et al. French 2010–2011 measles outbreak in adults: report from a Parisian teaching hospital. *Clin Microbiol Infect* 2014;20(4):O242–O244.
 44. Atmar RL, Englund JA, Hammill H. Complications of measles during pregnancy. *Clin Infect Dis* 1992;14(1):217–226.
 45. Rafat C, Klouche K, Ricard JD, et al. Severe measles infection: the spectrum of disease in 36 critically ill adult patients. *Medicine (Baltimore)* 2013;92(5):257–272.
 46. Farrag MA, Almajhdi FN. Human respiratory syncytial virus: role of innate immunity in clearance and disease progression. *Viral Immunol* 2016;29(1):11–26.
 47. Jain S, Williams DJ, Arnold SR, et al. Community-acquired pneumonia requiring hospitalization among U.S. children. *N Engl J Med* 2015;372(9):835–845.
 48. Johnstone J, Majumdar SR, Fox JD, Marrie TJ. Human metapneumovirus pneumonia in adults: results of a prospective study. *Clin Infect Dis* 2008;46(4):571–574.
 49. Seo S, Gooley TA, Kuypers JM, et al. Human metapneumovirus infections following hematopoietic cell transplantation: factors associated with disease progression. *Clin Infect Dis* 2016;63(2):178–185.
 50. Godet C, Le Goff J, Beby-Defaux A, et al. Human metapneumovirus pneumonia in patients with hematological malignancies. *J Clin Virol* 2014;61(4):593–596.
 51. Liu Q, He B, Huang SY, Wei F, Zhu XQ. Severe fever with thrombocytopenia syndrome, an emerging tick-borne zoonosis. *Lancet Infect Dis* 2014;14(8):763–772.
 52. Yu XJ, Liang MF, Zhang SY, et al. Fever with thrombocytopenia associated with a novel bunyavirus in China. *N Engl J Med* 2011;364(16):1523–1532.
 53. Takahashi T, Maeda K, Suzuki T, et al. The first identification and retrospective study of severe fever with thrombocytopenia syndrome in Japan. *J Infect Dis* 2014;209(6):816–827.

54. Kim KH, Yi J, Kim G, et al. Severe fever with thrombocytopenia syndrome, South Korea, 2012. *Emerg Infect Dis* 2013;19(11):1892–1894.
55. Oh WS, Heo ST, Kim SH, Choi WJ, Han MG, Kim JY. Plasma exchange and ribavirin for rapidly progressive severe fever with thrombocytopenia syndrome. *Int J Infect Dis* 2014;18:84–86.
56. Schountz T, Prescott J. Hantavirus immunology of rodent reservoirs: current status and future directions. *Viruses* 2014;6(3):1317–1335.
57. Manigold T, Vial P. Human hantavirus infections: epidemiology, clinical features, pathogenesis and immunology. *Swiss Med Wkly* 2014;144:w13937.
58. Papa A, Vaheeri A, LeDuc JW, et al. Meeting report: Tenth International Conference on Hantaviruses. *Antiviral Res* 2016;133:234–241.
59. Boroja M, Barrie JR, Raymond GS. Radiographic findings in 20 patients with Hantavirus pulmonary syndrome correlated with clinical outcome. *AJR Am J Roentgenol* 2002;178(1):159–163.
60. Rewar S, Mirdha D, Rewar P. Treatment and prevention of pandemic H1N1 influenza. *Ann Glob Health* 2015;81(5):645–653.
61. Nakajima N, Sato Y, Katano H, et al. Histopathological and immunohistochemical findings of 20 autopsy cases with 2009 H1N1 virus infection. *Mod Pathol* 2012;25(1):1–13.
62. Taubenberger JK, Morens DM. The pathology of influenza virus infections. *Annu Rev Pathol* 2008;3(1):499–522.
63. Agarwal PP, Cinti S, Kazerooni EA. Chest radiographic and CT findings in novel swine-origin influenza A (H1N1) virus (S-OIV) infection. *AJR Am J Roentgenol* 2009;193(6):1488–1493.
64. Oikonomou A, Müller NL, Nantel S. Radiographic and high-resolution CT findings of influenza virus pneumonia in patients with hematologic malignancies. *AJR Am J Roentgenol* 2003;181(2):507–511.
65. Marchiori E, Zanetti G, D'Ippolito G, et al. Swine-origin influenza A (H1N1) viral infection: thoracic findings on CT. *AJR Am J Roentgenol* 2011;196(6):W723–W728.
66. Ajlan AM, Quiney B, Nicolaou S, Müller NL. Swine-origin influenza A (H1N1) viral infection: radiographic and CT findings. *AJR Am J Roentgenol* 2009;193(6):1494–1499.
67. Wright PF, Kirkland KB, Modlin JF. When to consider the use of antibiotics in the treatment of 2009 H1N1 influenza-associated pneumonia. *N Engl J Med* 2009;361(24):e112.
68. Qureshi NR, Hien TT, Farrar J, Gleeson FV. The radiologic manifestations of H5N1 avian influenza. *J Thorac Imaging* 2006;21(4):259–264.
69. Galante O, Avni YS, Fuchs L, Ferster OA, Almog Y. Coronavirus NL63-induced adult respiratory distress syndrome. *Am J Respir Crit Care Med* 2016;193(1):100–101.
70. Geller C, Varbanov M, Duval RE. Human coronaviruses: insights into environmental resistance and its influence on the development of new antiseptic strategies. *Viruses* 2012;4(11):3044–3068.
71. Imai Y, Kuba K, Rao S, et al. Angiotensin-converting enzyme 2 protects from severe acute lung failure. *Nature* 2005;436(7047):112–116.
72. Hui DS, Memish ZA, Zumla A. Severe acute respiratory syndrome vs. the Middle East respiratory syndrome. *Curr Opin Pulm Med* 2014;20(3):233–241.
73. Cleri DJ, Ricketti AJ, Vernaleo JR. Severe acute respiratory syndrome (SARS). *Infect Dis Clin North Am* 2010;24(1):175–202.
74. Ooi GC, Khong PL, Müller NL, et al. Severe acute respiratory syndrome: temporal lung changes at thin-section CT in 30 patients. *Radiology* 2004;230(3):836–844.
75. Wong KT, Antonio GE, Hui DS, et al. Severe acute respiratory syndrome: radiographic appearances and pattern of progression in 138 patients. *Radiology* 2003;228(2):401–406.
76. Mackay IM, Arden KE. MERS coronavirus: diagnostics, epidemiology and transmission. *Virol J* 2015;12(1):222.
77. Al-Tawfiq JA, Zumla A, Memish ZA. Coronaviruses: severe acute respiratory syndrome coronavirus and Middle East respiratory syndrome coronavirus in travelers. *Curr Opin Infect Dis* 2014;27(5):411–417.
78. Ajlan AM, Ahvad RA, Jamjoom LG, Alharthy A, Madani TA. Middle East respiratory syndrome coronavirus (MERS-CoV) infection: chest CT findings. *AJR Am J Roentgenol* 2014;203(4):782–787.
79. Das KM, Lee EY, Al Jawder SE, et al. Acute Middle East respiratory syndrome coronavirus: temporal lung changes observed on the chest radiographs of 55 patients. *AJR Am J Roentgenol* 2015;205(3):W267–W274.
80. Choi WJ, Lee KN, Kang EJ, Lee H. Middle East respiratory syndrome-coronavirus infection: a case report of serial computed tomographic findings in a young male patient. *Korean J Radiol* 2016;17(1):166–170.
81. Choi SH, Hong SB, Kim T, et al. Clinical and molecular characterization of rhinoviruses A, B, and C in adult patients with pneumonia. *J Clin Virol* 2015;63:70–75.
82. Mermond S, Zurawski V, D'Ortenzio E, et al. Lower respiratory infections among hospitalized children in New Caledonia: a pilot study for the Pneumonia Etiology Research for Child Health project. *Clin Infect Dis* 2012;54(Suppl 2):S180–S189.
83. Choi SH, Huh JW, Hong SB, et al. Clinical characteristics and outcomes of severe rhinovirus-associated pneumonia identified by bronchoscopic bronchoalveolar lavage in adults: comparison with severe influenza virus-associated pneumonia. *J Clin Virol* 2015;62:41–47.
84. Kennedy JL, Turner RB, Braciale T, Heymann PW, Borish L. Pathogenesis of rhinovirus infection. *Curr Opin Virol* 2012;2(3):287–293.
85. Snoeck R, De Clercq E. Role of cidofovir in the treatment of DNA virus infections, other than CMV infections, in immunocompromised patients. *Curr Opin Investig Drugs* 2002;3(11):1561–1566.
86. Razonable RR. Antiviral drugs for viruses other than human immunodeficiency virus. *Mayo Clin Proc* 2011;86(10):1009–1026.
87. Kramer SC, Bansal S. Assessing the use of antiviral treatment to control influenza. *Epidemiol Infect* 2015;143(8):1621–1631.
88. Hung IFN, To KKW, Chan JFW, et al. Efficacy of clarithromycin-naproxen-oseltamivir combination in the treatment of patients hospitalized for influenza A(H3N2) infection: an open-label randomized, controlled, phase IIb/III trial. *Chest* 2017;151(5):1069–1080.